

Singapore's Zero-Energy Building's daylight monitoring system

Lars O. Grobe^{a)*}, Stephen Wittkopf^{a)}, Anupama Rana Pandey^{a)} and Yang Xiaoming^{a)}

Ang Kian Seng^b

Jean-Louis Scartezzini^{c)}

Stephen Selkowitz^{d)}

a) Solar Energy Research Institute of Singapore (SERIS), 7 Engineering Drive 1, Block E3A, #06-01, Singapore 117574, lars.grobe@nus.edu.sg^{a)*}, +6565151507 phone +6567751943 fax

b) Building and Construction Authority (BCA), 5 Maxwell Rd., #16-00 Tower Block MND Complex, Singapore 069110

c) Solar Energy and Building Physics Laboratory (LESO), Swiss Federal Institute of Technology Lausanne (EPFL), Batiment LE, Station 18, CH-1015 Lausanne, Switzerland

d) Environmental Energy Technology Division, Lawrence Berkeley National Laboratory, 1 Cyclotron Road, Berkeley, 94720 California, USA

1. Abstract

A setup to monitor the daylighting performance of different glazing types in Singapore is presented. The glazing is installed in the facade of four dedicated testing chambers in BCAA's Zero Energy Building in Singapore. These test rooms are equipped with sensors that both record illuminances on the work plane, and luminances as seen by occupants. The physical and logical design of the monitoring system is presented. Criteria to assess the daylighting performance are introduced, and initial results of the work in progress are presented.

Keywords: *daylighting, building monitoring system, glazing performance*

2. Introduction

The Zero Energy Building (ZEB) aims at demonstrating the application of various green building features, from Building-Integrated Photovoltaics (BIPV)^[1] to daylighting, solar cooling and green facade technologies. It allows test-bedding under realistic tropical conditions. Visitors can learn about the performance and benefits of different glazing types in the visitor centre attached to the ZEB^[2]. They can experience them by visiting the installations or accessing the building monitoring system (BMS). The BMS can be accessed using either the displays on site or by visiting the dedicated web-site.

The visitors will also complement the measured data by providing subjective feed-back through surveys. Both, the feed-back from the user-experience and the monitoring data will provide new insight into visual comfort and the performance of glazing under the specific climate conditions of the tropics in Singapore.

The four testing chambers are located on the ground floor of the ZEB facing west. They make up one third of the ground floor's west facade. Each chamber provides a floor area of about 13m² and is to approximate a standard office. The chambers are not air-conditioned and are separated by moveable walls. This enables visitors to directly compare all four glazing configurations side by side when open, but isolates the chambers from each other during measurements. The chambers' facade is almost completely glazed, with a 50cm high parapet. The glazing is implemented as a mullion/transom facade with inserted frames. The frames allow to reconfigure the facade using identical modules, and thus to modify the layout during the study.

Accepted manuscript. Please reference as:

Grobe, L. O., Wittkopf, S., Rana Pandey, A., Xiaoming, Y., Kian Seng, A., Scartezzini, J. L., & Selkowitz, S. (2010). Singapore's Zero-Energy Building's daylight monitoring system. In: *International Conference on Applied Energy*, Singapore.



Figure 1: Facade as seen from inside with partition walls opened. From left to right: glazing integrated blinds, electrochromatic glazing, aSi photovoltaic glazing, and clear glass.

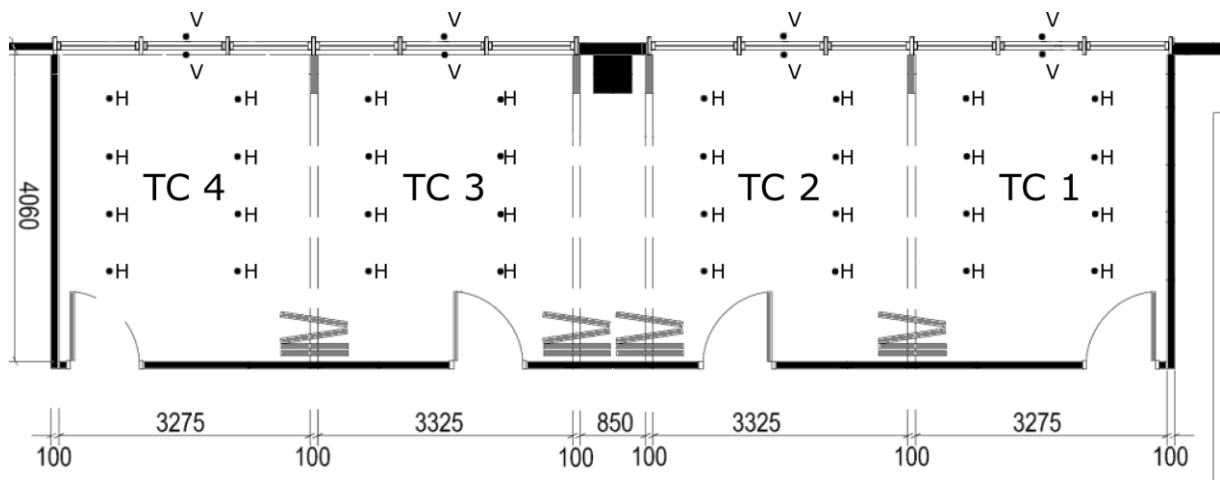


Figure 2: Layout of testing chambers with horizontal (H) and vertical (V) illuminance sensor positions.

All four glazing considered in the scope of this study are configured as double-glazing hold by frames. The total glazing thickness is identical for all four types and defined by the requirement of the electrochromatic glazing type. While the frames are mounted to the facade in a way that allows to swap them and thus combine the different glazing types in one chamber's facade, for this study each testing chamber corresponds to one type of glazing. The configurations of the testing chambers' facades for this study and their specifications are given in table 1.

location	glazing type	transmission vis. light [%]	reflectance vis. light [%]	Shading coeff. (max.)	u-value [W / (m ² K)]
TC 1	clear glazing	70	10	0.46	1.6
TC 2	aSi photovoltaic glazing	10	15	0.12	1.2
TC 3	electrochromatic glazing, untinted	62	15	0.55	0.28
	electrochromatic glazing, tinted	4	5	0.1	0.28
TC 4	glazing integrated blinds, open	68	15	0.75	1.4
	glazing integrated blinds, closed	5	15	0.23	1.4

Table 1: Glazing specifications for testing chamber TC 1-4.

3. Monitoring system set-up

The monitoring system consists of two types of sensors and data acquisition systems. The first type of sensors is integrating all incoming light over a hemisphere to derive the illuminance on a plane. The second group of sensors performs an angular resolved measurement, resulting in luminance maps.

3.1. Illuminance sensors

To assess the performance of facades for energy savings due to replacing electrical lighting by daylight, illuminance data needs to be acquired to compute the necessary contribution by electrical lighting.

As illuminance sensors allow readings only at one location each, the space needs to be divided into zones, with increasing distances to the window^[3, 4]. Each testing chamber is monitored by an array of eight horizontal illuminance sensors. The sensors, distributed on a regular grid and pointing up, measure the illuminance on a horizontal plane at 0.85m height. In each chamber, one additional illuminance sensor is pointing towards the glazing at 1.20m height, recording the illuminance on a vertical plane at the eye level of a seated occupant.

Exterior illuminance is monitored continuously by one sensor on the roof pointing up and one exterior sensor on the outside of the facade, pointing away from the building. This allows deriving daylight factors by relating interior to exterior horizontal illuminances.

The illuminance sensors closely follow the spectral luminous efficiency function for photopic vision^[5] as defined by the CIE. They are configured for a measurement range from 0 to 30,000lx, which is translated to a voltage of 0-30mV. The sensors are directly connected to a signal transmitter, which is linked to a 12bit controller that translates the analogue into a digital signal. This digital signal is fed into the central Building Management System and recorded. For the given illuminance range, the set-up allows illuminance reading in 10lx steps. The illuminance data is recorded in intervals of five minutes during 24 hours. The exterior illuminance sensors follow this set-up but are configured for an illuminance range of 0 to 150,000lx.

The results presented here were derived from a slightly changed setup, in which only readings from five of the horizontal illuminance sensors were recorded. Vertical illuminance was recorded neither inside the testing chambers nor outside.

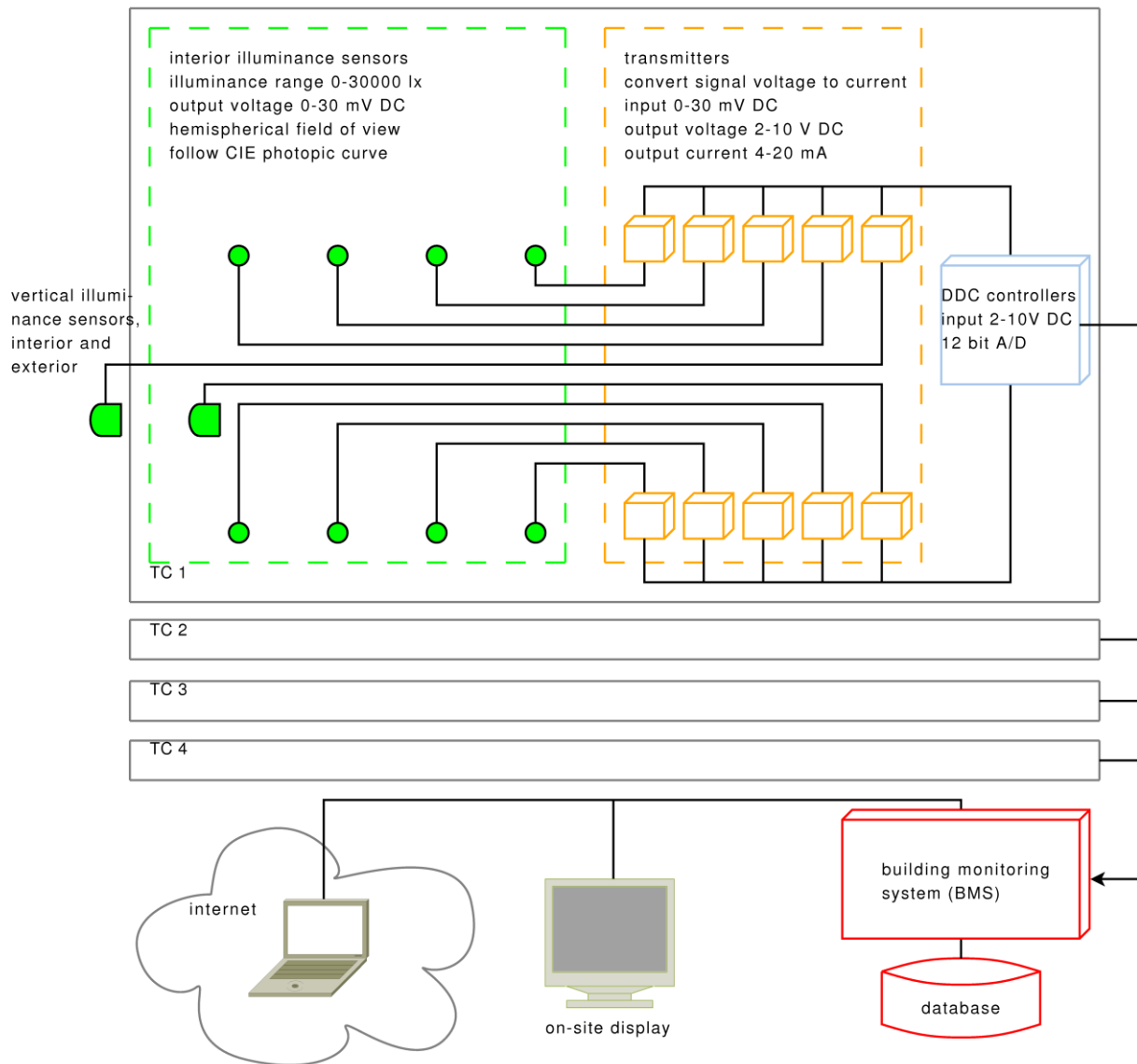


Figure 3: Layout of the illuminance monitoring system.

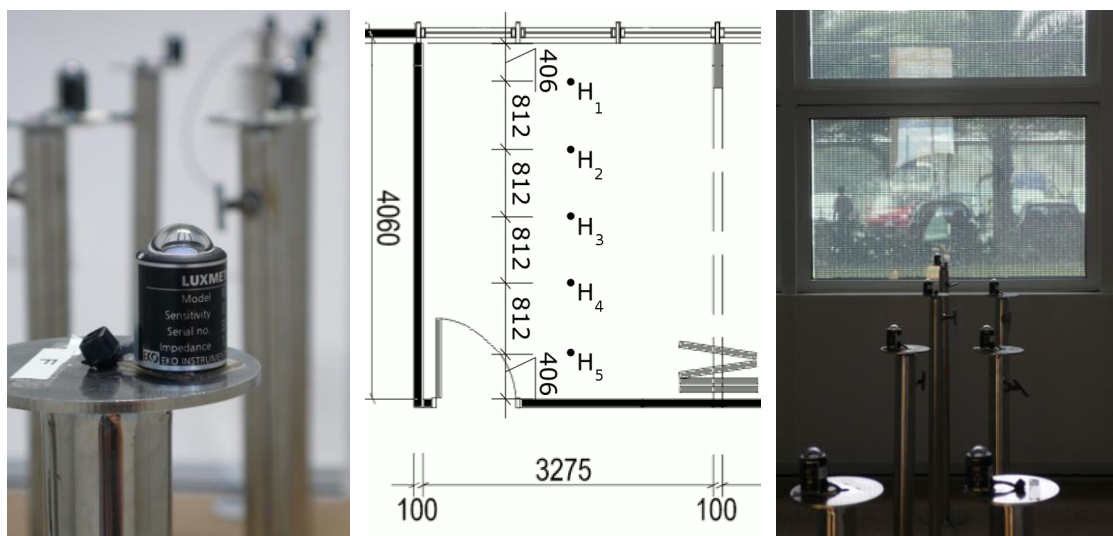


Figure 4: Horizontal illuminance sensors (left to right): close-up, modified sensor layout for daylight autonomy study, sensors in testing chamber 2 (only one row considered for the study)

3.2. High Dynamic Range imaging setup

Four digital single-lens reflex (DSLR) cameras, one in each chamber, mounted on tripods at 1.4m height and equipped with fisheye-lenses, are connected to a control computer using USB connections. The lenses, that cover more then the full hemisphere, show very little light fall-off towards the edges^[6].

$$(1) \quad EV \text{ span} = \log_2(\text{contrast ratio})$$

Once every ten minutes, a series of six exposures in 2EV steps is acquired from each camera. The exposure times are 0.1250s, 0.0333s, 0.008s, 0.002s, 0.0005s, 0.0002s. This scope from 1/8s to 1/5000s is equivalent to a range of more then 15 EV, when a range of 6 EV is considered for the sensor. This can be translated to a contrast ratio greater then 1:30000 according to formula 1. The range can be chosen according to the application needs, as long as the camera is capable of the settings. An open source library of tools to interface digital cameras called gphoto2^[7] was used, and as such the system could be adapted to use any of the many supported camera models.

After the transfer from the camera, which is based on standard USB cabling, the images are assembled into High Dynamic Range (HDR) images^[8] on the control pc. The open software library pfstools is used to derive camera response curves from captured image series, to calibrate and assemble the images into HDR images which provide valid luminance readings^[9]. The HDR images are encoded in the Radiance RGBE format^[10], which allows a high dynamic range at moderate storage requirements. The black frame resulting from the use of a circular fisheye lens with a rectangular sensor is cut off the image using Radiance's image processing tools^[11], and then named according to time and camera.

A system consisting mainly of Perl-scripts calling the different tools of the mentioned libraries has been developed that works independent from user interaction in both acquiring, processing and archiving the images. An external hard-disk is used to transfer the assembled HDR images, the synchronization starts automatically when the disk gets attached. Further processing of the imaging data happens off-site.

As all the program logic required for acquisition and processing is on the control computer, little requirements apply to the cameras other then the availability of suitable lenses and support by the software tools. This allowed setting up the system using consumer-grade DSLRs.

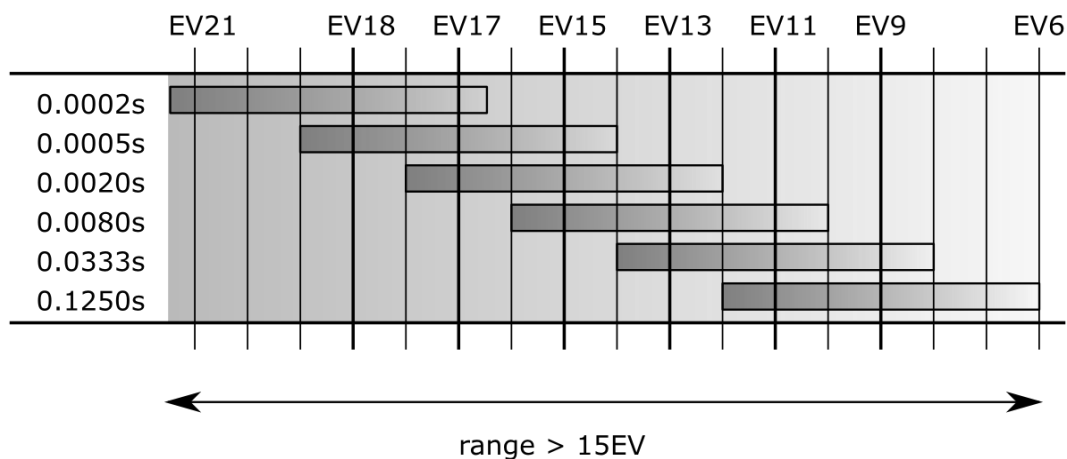


Figure 5: Overlapping luminance ranges of six low dynamic range exposures allow capturing a range of more then 15 EV when assembled into one high dynamic range image.

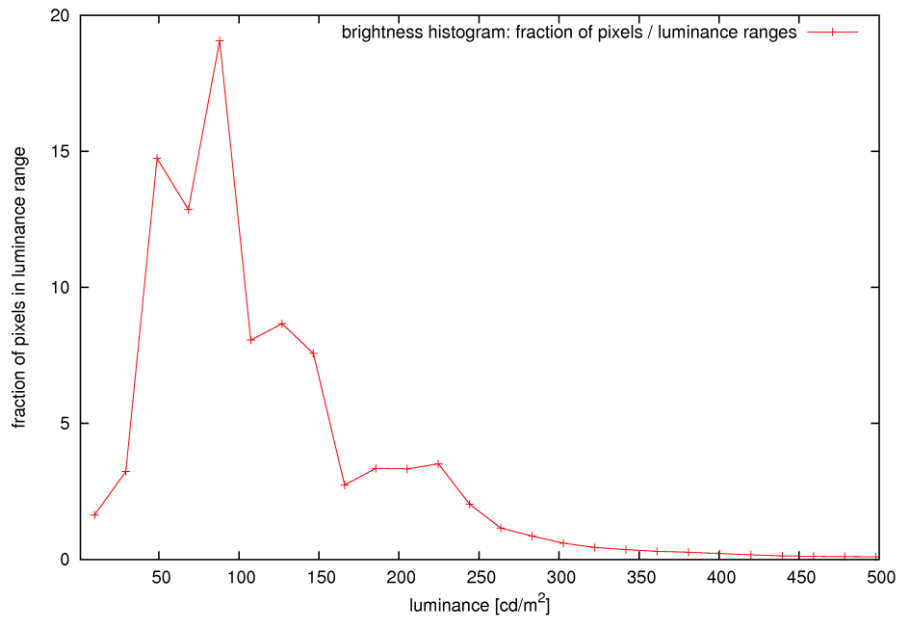


Figure 6: Typical histogram of a resulting high dynamic range image. The black pixels surrounding the circular are exposed where masked using image processing techniques.

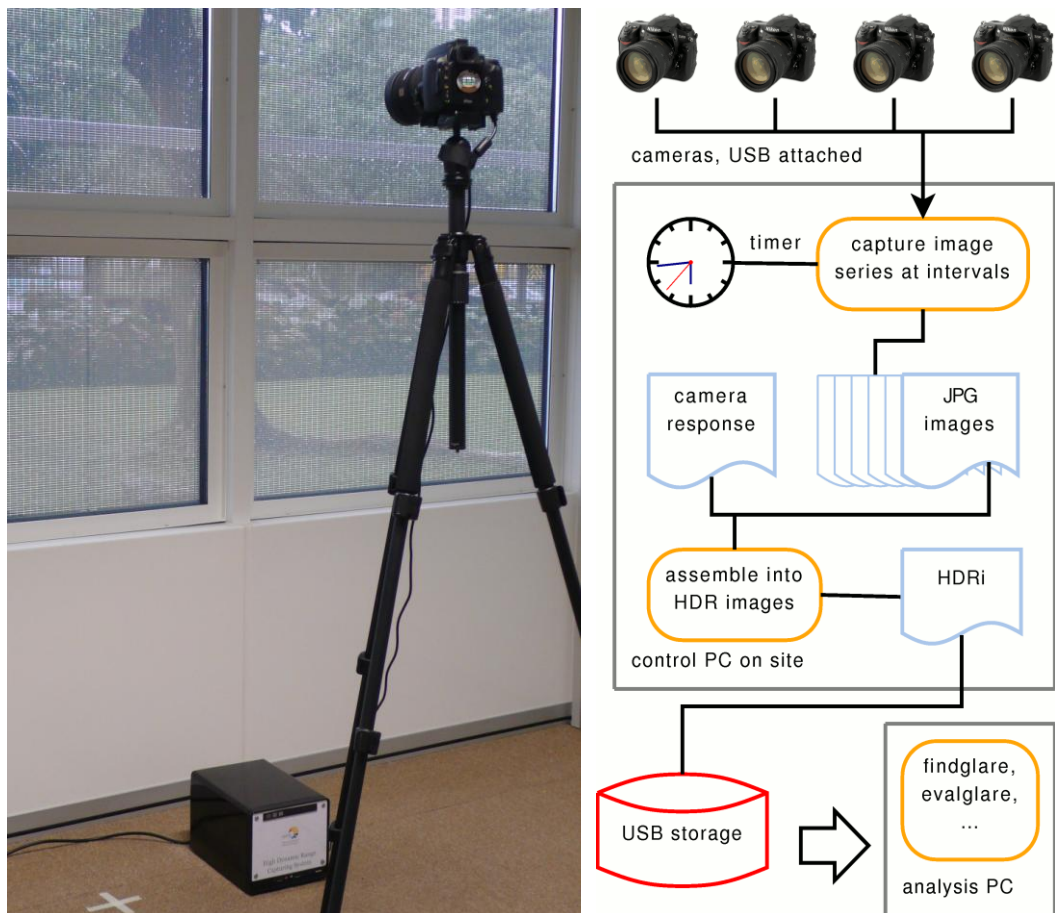


Figure 7: Automized high dynamic range imaging setup. One out of four cameras connected to the control pc (left), schematic overview of the setup including the processing steps (right).

4. Criteria for assessing daylighting performance

Two aspects of daylighting performance are covered by this study. The first one quantitatively describes the potential for energy savings, the second one is qualitative and focuses on user acceptance and visual comfort:

- 1) - Daylight Factor DF
- Useful Daylight Illuminance UDI
- Daylight Autonomy DA
- 2) - Vertical Illuminance
- IES Daylight Glare Index DGI
- Daylight Glare Probability DGP

Established performance indicators are illuminance levels on the work plane, and derived from that the daylight factor which does not take into account local climate conditions and occupancy requirements. As such, they have been proven to be limited for the assessment of daylighting designs. The possibility to consider climate data in computational simulations led to new performance indicators. The Useful Daylight Illuminance^[12] (UDI) relates the illuminance on the work plane to maximum and minimum thresholds. To achieve any relevant contribution to lighting of a space, a minimum of 100lx is set, while an illuminance of more than 2000lx is considered as affecting the occupants. This results in three metrics for the UDI, defining exceeding (>2000lx), insufficient (<100lx) and achieved requirements (100-2000lx).

To describe the potential for energy savings in lighting, the daylight autonomy of each testing chamber is proposed for initial studies^[13]. This requires knowledge on the required illuminance as well as representative data on the average illuminances achieved over the occupancy period. A daily occupancy period from 8 a.m. to 6 p.m. is typically to be considered for offices. Building codes in Singapore require 300 lx to 500 lx for office work^[14]. The study assumes a baseline illuminance requirement as of 300 lx accordingly at a working plane level of 0.85m. The daylight autonomy is derived as the fraction of occupancy time that illuminance measured by the sensors meets this requirement for the monitored time span.

The assessment of visual comfort and glare requires assumptions on the field of view of the occupant. Different glare indices are established, mostly based on empirical studies from surveys, for different environments. In the scope of this study, the software tool findglare (from the Radiance lighting simulation environment) was applied both on HDR images captured on site and on synthetic HDR images from simulation. The performance indicator used was the Daylight Glare Index (DGI)^[15] as defined by the IES glare formula:

$$(2) \quad DGI = \sum_{i=1}^n \frac{L_s^{1.6} \cdot \Omega^{0.8}}{L_b + 0.07 \cdot \omega^{0.5} \cdot L_s}$$

L_s : source luminance [cd/m^2]

ω : angular size of the source as seen by the observer [sr]

L_b : background luminance [cd/m^2]

Ω : solid angle subtended by the source, modified for the effect of the position of the observer in relation to the source [sr]

The glare indices presented reflect the exposure to glare for an observer facing the facade. The IES DGI does not consider a task area, and can thus be determined without further assumptions on occupant's behaviour or furnishing of the office spaces. The resulting value is compared to a look-up table, relating it to a grading system from just perceptible (≤ 16) to intolerable (> 28).

Recently, a new glare index referenced to as Daylight Glare Probability (DGP)^[16] had been proposed to address the specific characteristics of glare caused by daylighting. Existing indices had been found to lead to wrong results when assumptions typically valid for artificial lighting did not match the conditions in daylight spaces. Other than the DGI, which relies mostly on luminances (which tend to have a high variability for facades and thus to scatter in the results), it includes vertical illuminance. This index is calculated according to formula 3:

$$(3) \quad DGP = c_1 \cdot E_v + c_2 \cdot \log \left(1 + \sum_i \frac{L_{s,i}^2 \cdot \omega_{s,i}}{E_v^{a_1} \cdot P_i^2} \right) + c_3$$

E_v :	vertical eye illuminance [lm/m^2]	c_1 :	$5.87 \cdot 10^{-5}$
L_s :	luminance of source [cd/m^2]	c_2 :	$9.18 \cdot 10^{-2}$
ω_s :	solid angle of source [sr]	c_3 :	0.16
P :	position index []	a_1 :	1.87

The DGP directly describes the probability in per cent that a person will perceive glare. As not only the vertical illuminance as a less variable parameter for environments with outside view had been introduced, but also the high number of probants used to develop the index (74 for DGP), a higher consistency of predictions for daylight environment is expected.

5. Initial results

First acquired records were analyzed according to the defined daylight performance criteria. As daylight is subject to seasonal and random changes, projectable results require a monitoring period of at least a year, while the data used for the analysis shown here was acquired during short test runs of the system.

The measurement data for one day at TC 1 (clear glazing) is presented as an example of the raw data that is stored in the BMS' database. As the illuminance monitoring system does not work with a dynamic range, the matching of the components such as sensors, transmitters and DDC-converters was a critical step to achieve the resolution of 10lx over the wide range from 0 to 30,000lx. The cabling from the sensors to the DDC converter proved to have significant impact on the stability of the analog signal.

The logarithmic plot shows the readings from four sensors at TC 1 over one day, with the stable increase in the morning and sudden illuminance changes in the afternoon, when the sensors get directly hit by the sun. The noise at night for the three sensors located beyond 2m from the facade is due to the fact that these receive an illuminance below 10lx, which is the resolution of the system, resulting in random readings.

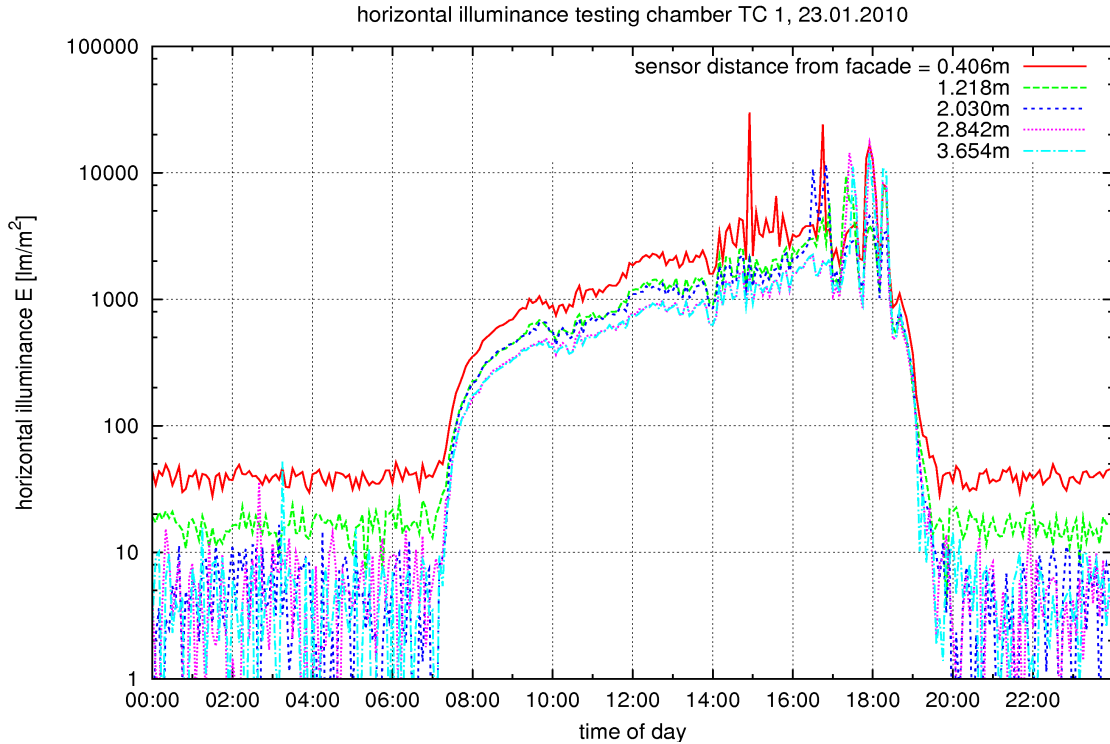


Figure 8: Logarithmic plot of four illuminance sensors' reading for one day at testing chamber TC 1 (clear glazing, facing west).

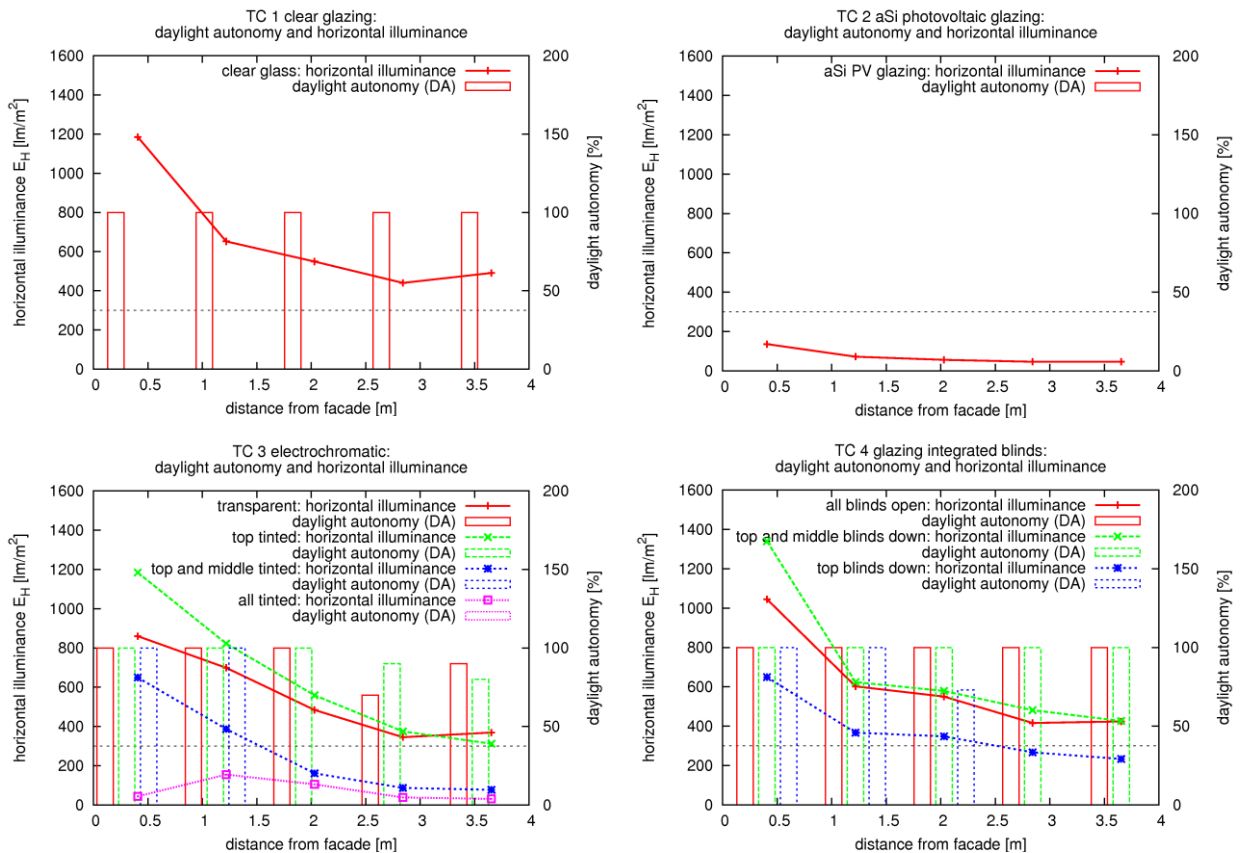


Figure 9: Horizontal illuminances and derived daylight autonomy percentages for four testing chambers TC1-4. In testing chamber TC 2 (photovoltaic glazing), daylight autonomy could not be reached at any measurement interval.

Daylight autonomy during daytime was easily achieved by clear glazing and glazing with integrated blinds, even when the blinds were closed. Under tropical climate conditions, the chambers located at the building perimeter are exposed to intense irradiation. The aSi PV facade does not achieve a transmittance to reach daylight autonomy at any time of the monitored period except for the position directly behind the glazing, when very high exterior illuminance was observed. Electrochromatic glazing could still achieve daylight autonomy levels of 40% during daytime when switched to clear, but dropped to 0% when switched to tinted. Besides being adaptable to the environmental conditions and still achieving sufficient illuminance levels at any time, glazing integrated blinds showed a potential to more evenly spread light into the room.

For each testing chamber, the results from capturing eight HDR images are presented here, covering two hours from 2 p.m. to 4 p.m. with an interruption of fifteen minutes at 3 p.m. The glare studies based on these HDR images resulted in acceptable glare indices except for the case of the glazing with open integrated blinds. Compared to the clear glass facade, significantly higher vertical illuminance was measured, and this may indicate that between the capturing times of the two HDR images, the exterior conditions had changed. The aSi PV facade of TC 2 leads to very low vertical illuminances and shows no potential for glare, while the electrochromatic glazing shows its ability to effectively bring down the glare index numbers by shading the testing chamber – however at the cost of very low illuminances. It has to be noted that the high sun elevation during the monitoring period does not allow direct visibility of the sun, and thus the assessment of the strongest potential source of glare is excluded here.

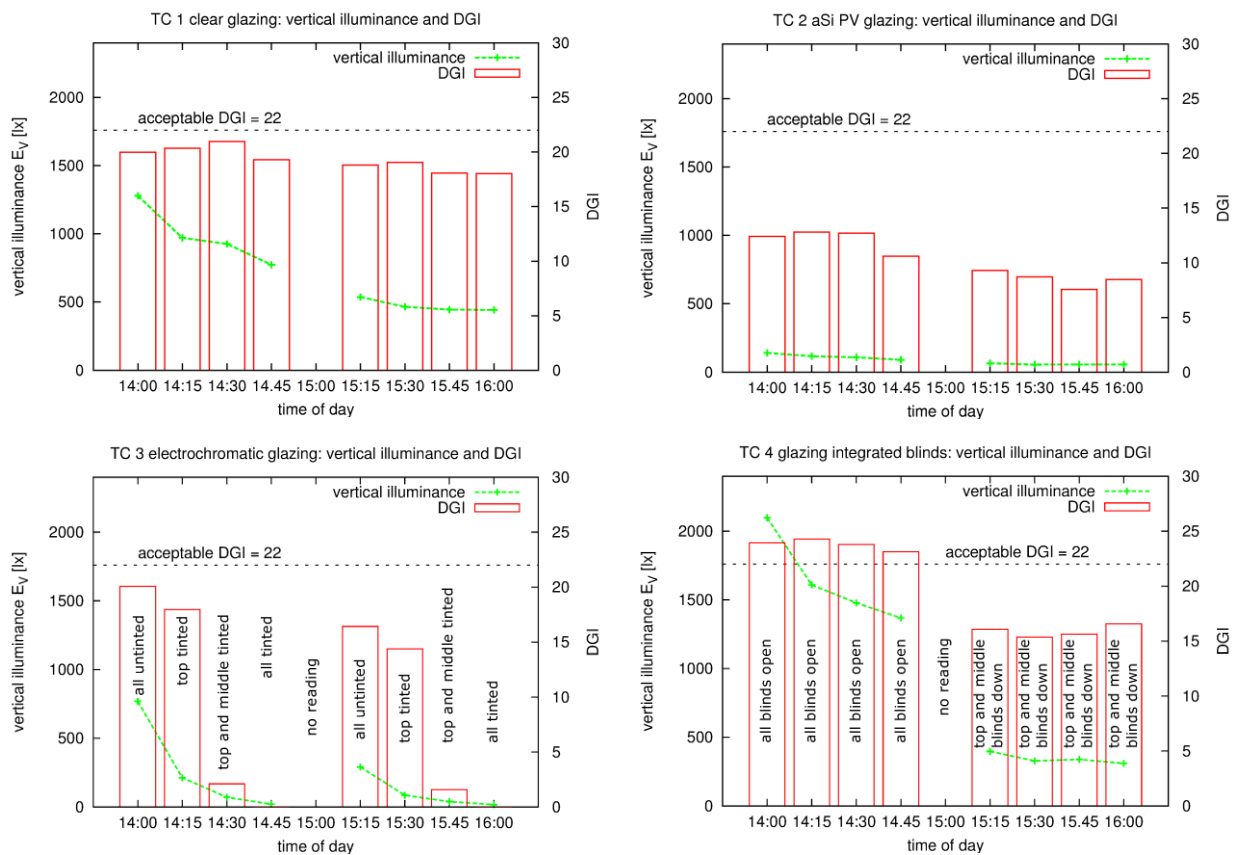


Figure 10: Vertical illuminance and glare indices according to CIE Daylight Glare Index (DGI) for a monitoring period of two hours at all testing chambers. Note that the electrochromatic glazing (TC 3) and glazing integrated blinds (TC 4) were operated during the monitoring, while transmissive properties for TC 1 and 2 were constant.

6. Discussion

Initial exemplary readings of the sensors were presented. As the system has just started to be operational, valid data from several sensors is still not available and not all daylighting performance metrics could be derived yet. E.g. without having readings from exterior sensors, the daylight factor cannot be calculated from given interior horizontal illuminances. Besides completeness of the readings, a sufficient monitoring time-span is required to acquire representative data. As such, the set-up of the daylight monitoring systems are presented more than the results.

The current monitoring system will be kept in operation for a full year to acquire enough data for representative results. Additional performance indicators, such as alternative glare indices, will be introduced. Current photometric monitoring will be complimented by refined radiometric measurements using CCD-spectrometers that also capture the effects of glazing types on colour rendition, their capability to block unwanted long-wavelength radiation and the changes in the daylight spectrum according to season and daytime. Furthermore, advanced daylighting systems such as horizontal light ducts, vertical light pipes and light shelves, installed both on the in- and outside of the facade, are studied. The data acquisition from sensors will be complimented by surveys to relate the numerical results of occupant experience and acceptance.

7. Acknowledgment

The presented work is a part of research project funded by the “Ministry of National Development Research Fund for the Built Environment” and Economic Development Board’s “Clean energy Research and Test-bedding” programme.

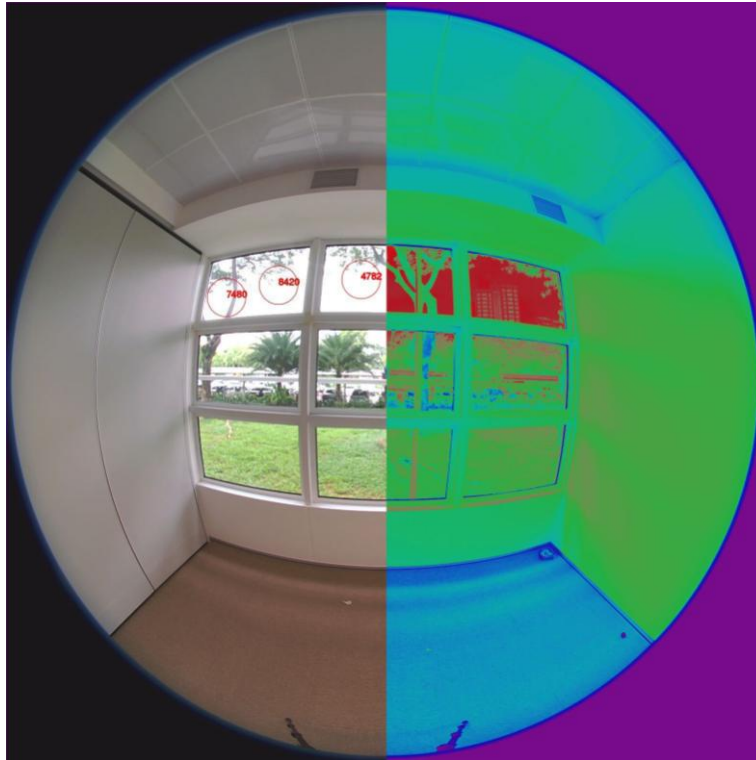


Figure 11: Tonemapped image derived from HDR image with glare sources as found by findglare (left), falsecolor showing the luminance distribution (right) at testing chamber TC 1 (clear glass).

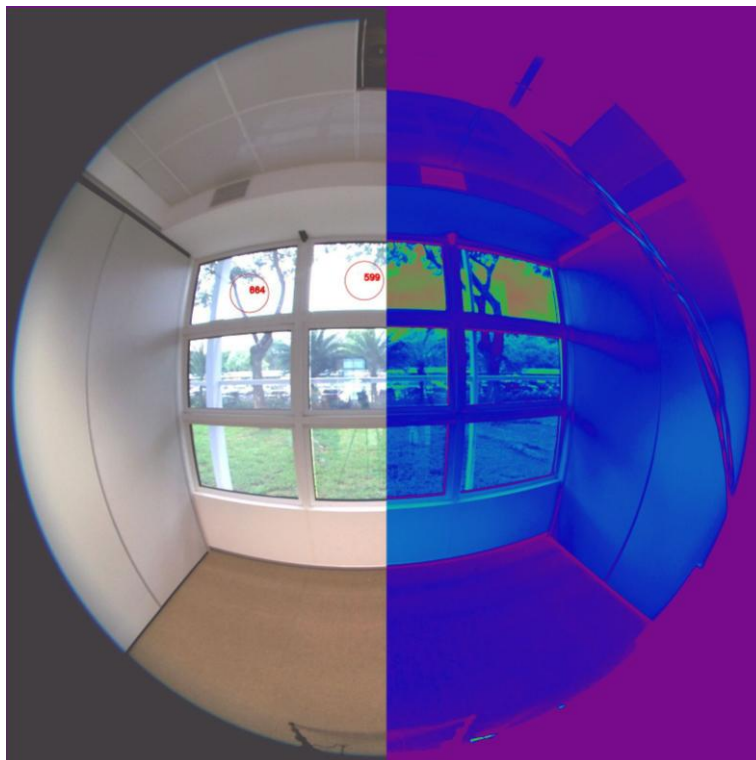


Figure 12: Tonemapped image derived from HDR image with glare sources as found by findglare (left), falsecolor showing the luminance distribution (right) at testing chamber TC 2 (aSi photovoltaic glazing).

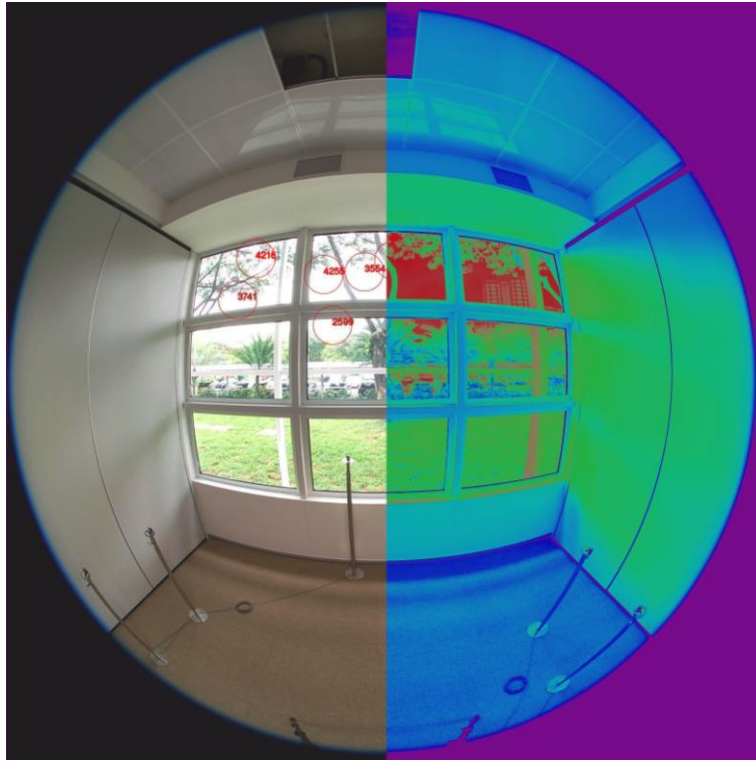


Figure 13: Tonemapped image derived from HDR image with glare sources as found by findglare (left), falsecolor showing the luminance distribution (right) at testing chamber TC 3 (electrochromatic glazing).

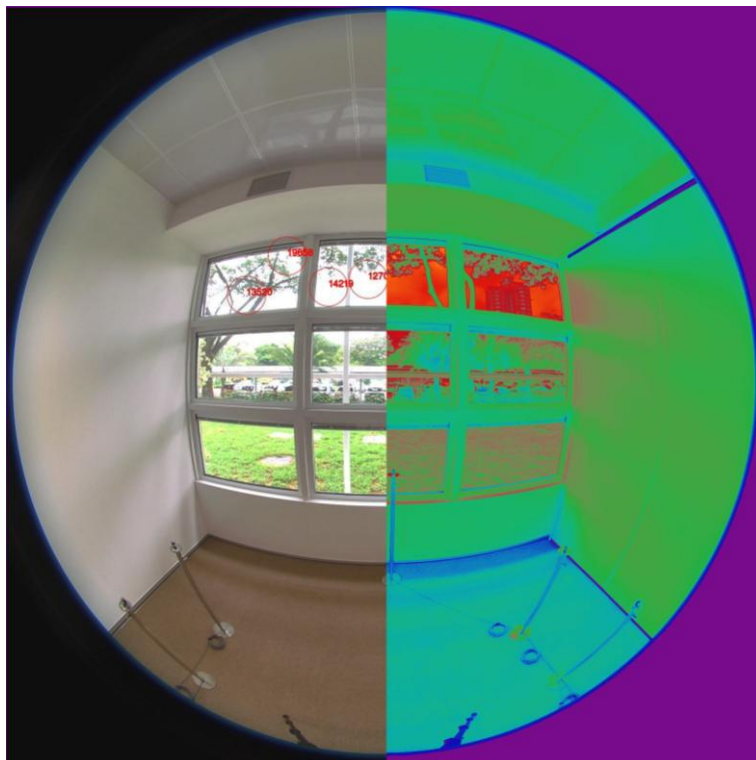


Figure 14: Tonemapped image derived from HDR image with glare sources as found by findglare (left), falsecolor showing the luminance distribution (right) at testing chamber TC 4 (glazing integrated blinds).

-
- [1] Wittkopf S, Seng AK, Poh P and Pandey A, BIPV Design for Singapore Zero-Energy Building, PLEA 2008 5th conference on passive and low energy architecture, Dublin, 2008.
 - [2] Wittkopf S, Pandey A, Grobe LO and Borsuit A, Demonstration and test bedding of four glazing types in daylight test chambers in Singapore, Proceedings of Glass Performance Days 2009, Tampere, 2009.
 - [3] Atif MR, Love JA and Littlefair P, Daylighting monitoring protocols & procedures for buildings, a report of IEA Task 21 / Annex 29, 1997.
 - [4] Velds M and Christoffersen J, Monitoring procedures for the assessment of daylighting performance of buildings, a report of IEA Task 21 / Annex 29, 2001.
 - [5] ISO 11664-1:2008(E)/CIE S 014-1/E:2006 CIE Standard Colorimetric Observers, Commission Internationale de l'Eclairage, 2006.
 - [6] Jacobs A, Wittkopf S and Grobe LO, Per-pixel sky luminance with HDR photography, 7th international Radiance Workshop, 2007.
 - [7] Meissner M, Figuiere H, Fritzinger S, Müller S and others, gphoto2, <http://www.gphoto.org>.
 - [8] Debevec PE and Malik J, Recovering high dynamic range radiance maps from photographs, Proceedings of SIGGRAPH 97, Computer Graphics Proceedings, Annual Conference Series, pp. 369-378, 1997.
 - [9] Krawczyk G, Mantiuk R and others, pfstools, <http://pfstools.sourceforge.net>.
 - [10] Ward G, Real pixels, Graphics Gems II, Ed. by J. Arvo, Academic Press, 1992.
 - [11] Ward G, Shakespeare R, Rendering with Radiance, pp. 17,18, 1998.
 - [12] Nabil A and Mardaljevic J, Useful daylight illuminance: a new paradigm for assessing daylight in buildings, Lighting Research and Technology, V. 37, No. 1, pp. 41-57, 2005.
 - [13] Reinhart CF, Mardaljevic J and Rogers Z, Dynamic daylight performance metrics for sustainable building design, Leukos V. 3, No. 1, pp. 1-25, 2006.
 - [14] SS 531 – 1:2006 Code of practice for lighting of work places – Indoor, Electrical and Electronic Standards Committee, 2006.
 - [15] The development of the IES glare index system, Transactions of the Illumination Engineering Society, V. 27, No. 1, pp. 9-26, 1962.
 - [16] Wienold J and Christoffersen J, Evaluation methods and development of a new glare prediction model for daylight environments with the use of CCD cameras, Energy and buildings, V. 38, No. 7, pp. 743-757, 2006.